A Laboratory Analysis of the Effect of Macropores on Solute Transport

by D. Wildenschild[a], K. H. Jensen[a], K. Villholth[a], and T. H. Illangasekare[b]

Abstract

Macropores play an important role in many soils in relation to ground-water contamination by providing preferential pathways from the root zone to the water table. Surface-applied agrochemicals may hereby be carried quickly to the shallow ground water. The reduced retention combined with a small contact area between the flowing water and the soil implies that little removal from physical, chemical, and microbiological processes may take place, thus increasing the risk of ground-water contamination.

A laboratory procedure for evaluating the effect of macropores in a given soil is proposed and tested. The procedure involves the following sequence of experiments on two undisturbed soil monoliths: (1) measurements of the distribution of outflow, (2) measurements of breakthrough curves, (3) dye application for visual observation of macropores; and (4) horizontal slicing of the monoliths to measure macropore distribution and continuity of macropores. The experimental procedure is based on well-documented techniques that combined will provide evidence on the significance of macropores in relation to ground-water contamination and guidance for selecting the appropriate model for simulating flow and transport at the field in question.

The laboratory procedure was tested on two large, undisturbed soil monoliths (30 cm in diameter) removed from the unsaturated zone at a clayey moraine agricultural field in Denmark. This soil was known to have many macropores. The investigations documented the strong influence of these structures on flow and transport suggesting that a traditional flow and transport model would be inadequate for simulating the processes occurring in the field.

Introduction

In recent years, much attention and concern have been given to the problems associated with contaminant transport to surface-water and ground-water systems. Of particular concern is the leaching of nutrients and pesticides to ground water, because high concentrations of these constituents make the ground water unsuitable for drinking-water supply. Other unsaturated zone sources arising from buried waste products or spills may similarly give rise to contamination problems. Thus, an understanding of the mechanisms that control the transport and residence time of chemicals in the unsaturated zone is important.

In general, it is difficult to predict water and solute transport in subsurface systems due, in part, to the complicated heterogeneous composition of natural soil formations. The difficulty is compounded in soils that contain preferential flow pathways due to the presence of cracks, fissures, structural peds, wormholes, and root channels (see e.g. Thomas and Phillips, 1979; Beven and Germann, 1982; White, 1985).

The presence of macropores may, under certain conditions, cause the dissolved matter to bypass the soil matrix, and transport will take place in a comparatively small part of the porous medium. This bypassing causes a very fast initial penetration of solutes through the vadose zone followed by an asymmetrical "tailing" caused by diffusive mass transfer of solutes between macropores and soil matrix (see Brusseau and Rao, 1990).

Several laboratory studies have documented the effect of macropores and shown that the residence time is far too short to be accounted for by a simple displacement theory. Anderson and Bouma (1977a, b) were among the first to produce breakthrough curves in the laboratory on undisturbed aggregated soil columns showing bypass flow. Bouma and Anderson (1977) also showed the effect of preferential flow on prepared soil columns with artificially drilled vertical channels. Later laboratory experiments on undisturbed soil columns by Tyler and Thomas (1981), and White et al. (1984) have confirmed that the maximum effluent concentration of the chloride tracer appears ahead of the time required to replace one pore volume. McMahon and Thomas (1974) compared undisturbed and disturbed columns, and showed that both chloride and tritiated water appeared to have moved much further in the undisturbed columns than in the disturbed ones, suggesting a consider-

[a]Institute of Hydrodynamics and Hydraulic Engineering, Technical University of Denmark, Bldg. 115, DK-2800 Lyngby, Denmark.

[b]Department of Civil, Environmental, and Architectural Engineering, Campus Box 428, University of Colorado, Boulder, Colorado 80309.

Received April 1993, revised November 1993, accepted December 1993.

able bypassing of the soil by both water and chloride. Similar results were reported by Khan and Jury (1990). Kluitenberg and Horton (1990) examined the effect of the solute application method on preferential transport of solutes in soil columns. They showed that for initially drained macroporous soil a pulse application would result in very fast and only slightly diluted breakthrough of chloride, whereas a continuous drip application results in a slower increase in concentration and a peak that appears later than those obtained by the pulse experiments. They attributed the fast breakthrough in the pulse experiments to a comparatively larger contribution of continuous channels and voids to the transmission process in which the contact time for diffusion and advection of solute into the matrix is minimal.

Dye experiments have been carried out by Seyfried and Rao (1987), Ghodrati and Jury (1990), and Booltink and Bouma (1991) to visualize the preferential movement of water and solutes. Andreini and Steenhuis (1990) conducted experiments on grid lysimeters, and observed that the dyed flow paths led to the areas where water and solute exited the column.

Field experiments have been carried out where it has been possible to detect surface-applied substances at depths some times far in advance of what would agree with the displacement theory. Sampling has been made through subsurface drains (Everts et al., 1989; Van Ommen et al., 1989; and Villholth et al., 1991) porous suction cups (Jardine et al., 1990), and by coring (Ghodrati and Jury, 1992).

The experimental evidence cited above, and reviews by Beven and Germann (1982), White (1985), and van Genuchten and Jury (1987), suggest that the traditional one-domain advection-dispersion formulation is inadequate for describing solute transport in macroporous soil. Jarvis et al. (1991) and Wildenschild (1991) tested both one-domain and two-domain numerical models on data from experiments on macroporous soils and found that the one-domain formulation was unable to reproduce the observed leaching pattern.

Previous work has shown that macropore behavior is site-specific and depends on several circumstances including experimental boundary and initial conditions. The objective of the present study is to develop a general procedure for evaluating the existence and significance of macropore flow and transport in a given soil by combining different experimental techniques described in the literature. A key issue is that the procedure should provide guidance toward selection of a numerical model for simulating flow and transport in the particular soil. The procedure includes flow, tracer, and dye experiments on undisturbed soil monoliths installed in the laboratory. Contrary to most previous investigations, we propose to use large, undisturbed soil monoliths (30 cm in diameter, 50 cm in length) in an attempt to preserve the soil structure present in the field. The technique for collecting the monoliths in the field, the laboratory setup, and monitoring system are described in the paper, and the procedure is demonstrated on a soil typical of the eastern part of Denmark to assess the significance of macropore flow in this particular soil.

Experimental Procedures

Test Site

The experimental procedure was tested on two soil monoliths (denoted I and II) that were excavated near Viby on Sjælland, Denmark, from a location where field-scale tracer experiments were performed (Villholth et al., 1991). The laboratory experiments would thus provide complementary information to the ongoing field investigations. The area is part of a relatively flat moraine country with a glacial series consisting of 10-25 meters of clayey moraine with local horizons of coarser composition. The soil characteristics at the site were investigated from two excavation pits supplemented with soil samples from 28 hand-drilled bore holes. The soil is developed on a clay till with a clay fraction of 5-20% by weight, and can be characterized as a pseudo gley brown soil with visible gley development below approximately 80 cm indicating partly imperfect drainage. The boundary of the B-C horizons determined by soil structure and color is found at 90-150 cm depth, deepest where sandy till occurs. The upper limit of calcareous soil mostly follows the B-C horizon boundary. From the excavation pits, macropore structures as worm holes and root channels in the upper soil layers and fracture planes between peds of different order and size in the lower layers were observed. Worm holes and root channels observed in the field and when slicing the monoliths were predominantly cylindrical and vertical with typical diameters of 2-4 mm and a maximum of approximately 10 mm. The macropore intensity in the horizontal plane was approximately 15 per square decimeter. Some of the channels were continuous to a relatively large depth, in certain cases up to 1.3 m. Between the depths of 40 cm and 120 cm, distinct peds of 1-5 cm were seen.

Excavation Procedure

Two different methods of soil sampling have commonly been used to remove and isolate undisturbed soil samples, namely: (1) drilling-driving, or (2) hand excavation. The drilling-driving method involves a combination of drilling or driving in the sampling process. Following this method, a thin-walled cylinder with a sharpened bottom edge is driven into the soil by either applying weight at the top or using a drilling technique. This method has been employed by Persson and Bergström (1991), Brown et al. (1985), and Khan and Jury (1990), among others. The hand excavation method consists of isolating an undisturbed block of soil by hand, and then coating it with a sealant material to maintain the integrity of the sample. Once the sealant is dry, the undisturbed sample can be transported to the laboratory. This method has been used in investigations by Reeves and Beven (1990) and Andreini and Steenhuis (1990). This sampling technique requires that the soil is cohesive enough to allow the monolith to stand upright when it is coated with sealant. The hand-carving technique was chosen for our study because the soil fulfilled the above criteria, and we believe that this sampling technique causes the least disturbance during excavation and transport to the laboratory.

Before collection of the soil monoliths, two ditches

were initially dug by a backhoe to approximate depths of 130 cm at sampling points 120 cm apart. At the day of excavation the ground-water level was located deeper than the bottom of the pit. The monoliths were carved out by hand to a depth of 55 cm, initially as squares of 50 × 50 cm and later trimmed to the final shape of approximately 30 cm in diameter. The clayey moraine soil was quite compact, and the monoliths were easily carved out. No deformation of the monoliths was observed after having reduced the sidewall pressure. To create an impermeable boundary around the edges of the monoliths, they were wrapped in a plaster of paris bandage shortly after excavation, sealed with water-proof lacquer, and wrapped in plastic film. Finally, a PVC-casing, 42 cm in diameter and 53 cm high, was placed around the monoliths, and the resulting gap filled with plaster of paris. The plaster dried within approximately an hour, and the monoliths were then loosened at the base, sealed at both ends to prevent water loss, and transported carefully to the laboratory in upright position to minimize deformation.

Laboratory Setup Procedures

The experimental setup (Figure 1) for the controlled flow and tracer investigations consisted of a support base, constructed as a grid cell pattern to distribute water and solute into the partitioned collection system. A rain simulator, consisting of a dispenser and a peristaltic pump, was constructed to provide a controlled, constant intensity water supply uniformly distributed over the monolith surface. The dispenser for the rain simulator was made of a porous plastic material called Vyon F (thickness = 4.75 mm) manufactured by Porvair Ltd., U.K. The rain simulator was tested and calibrated directly on the collection system prior to the experiments and showed satisfactory distribution. A system of hoses and collecting bottles was placed beneath the monolith for collecting distributed amounts of water and solute during the experiments.

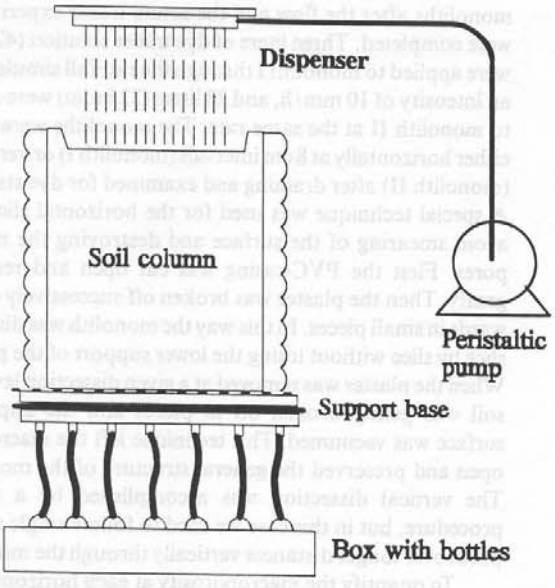

Fig. 1. Laboratory setup.

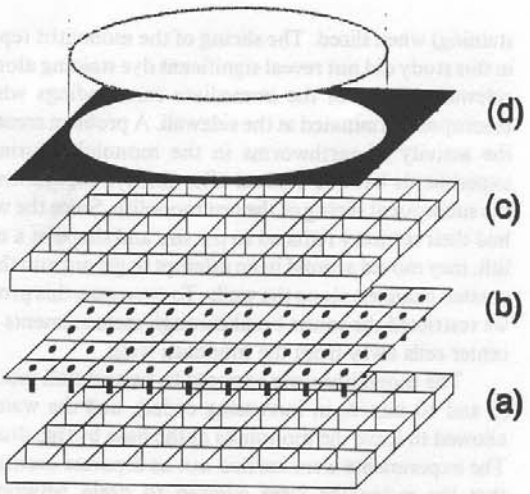

Fig. 2. Base setup for the monoliths. (a) and (c) stainless steel grids, (b) zinc plate with PVC tubes, (d) fine mesh with silicone strings.

The base was designed to facilitate measurements of outflow distribution in a grid constructed around a 45 × 45 cm stainless steel grid of approximately 2 cm height (Figure 2). The grid consisted of a 9 by 9 array of 5 cm square cells. This grid was attached to a zinc plate in which 5 × 5 cm grooves were stamped out so it would fit the grid. At the bottom of each hollow a hole was made, and a brass tube was soldered to the hole to which a PVC-tube was attached. A box with 69, 100 ml bottles was then placed beneath the grid system to collect the water. The number of tubes, and accordingly bottles, was reduced from 81 to 69 active collectors because the monoliths were circular (Figure 3). The zinc plate with the tubes was placed between two supporting stainless steel grids. The whole grid system was taped together, and all gaps were filled with silicone paste to avoid flow between the individual cells. On top of the upper grid, a fine mesh (100 μm) was placed to prevent fine particles from being washed out of the monolith and yet sufficiently permeable not to impede the flow. In addition, silicone strings were placed in a grid on top of the mesh according to the 9 by 9 array (Figure 2). When the monolith was placed on top of the strings, they would penetrate into the soil and prevent water from flowing laterally before dropping into the cells. This precaution was tested when the monoliths were dismounted from the base after the dye tracer experiments had been carried out. It was then verified visually that no cross-flow between cells had occurred. When the monolith and base were attached to each other, the whole system was lifted to the setup shown in Figure 1.

To prevent water and solute from flowing preferentially along the sidewalls during ponding, a hollow was dug in the top of the monoliths to a depth of 5 cm. The area to which water was supplied was hereby reduced to 28 cm diameter. A preliminary dye experiment on a soil test sample where this measure was not taken showed severe sidewall flow (dye

staining) when sliced. The slicing of the monoliths reported in this study did not reveal significant dye staining along the sidewalls except in the immediate surroundings where a macropore terminated at the sidewall. A problem created by the activity of earthworms in the monoliths during the experiments became evident after the dye experiment and the subsequent slicing of the test monolith. Since the worms had their territory reduced to the size and shape of a monolith, they moved around in an attempt to get out and thereby created channels along the walls. To overcome this problem, we restricted the solute breakthrough measurements to the center cells away from the monolith walls.

The monoliths were exposed to two rainfall intensities (5 and 10 mm/h, in increasing order), and the water was allowed to leave the monoliths at the base by free drainage. The experiments were carried out as separate events, such that the monoliths were allowed to drain between rain events. Only the second 10 mm/h event on monolith II followed shortly after the previous experiment without preliminary drainage. The flow distribution at the base was measured with an array of bottles, which were emptied every half hour and the amount weighed on a balance. After the flow distribution was determined, the solute tracer experiments were carried out to obtain solute breakthrough curves for the different application rates. Prior to solute application the monoliths were subjected to the selected rain intensity for a couple of days to assure full saturation and steady total outflow rate. During the flow and solute tracer experiments, the total outflow, or the outflow from a subset of cells, was measured continuously at one minute intervals at the bottom of the monoliths by one or two digital scales equipped with serial interfaces (RS232) for communication with a personal computer.

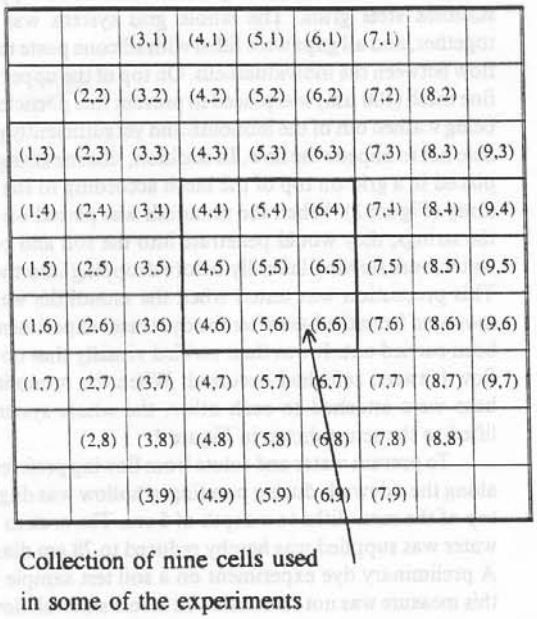

Fig. 3. Plan of the 69 cells monitored in the experiments.

When the total monolith outflow rate had reached steady state at the particular application rate, the solute tracer solution was carefully poured onto the soil surface as a slug. Following this pulse application, the solute concentration was measured continuously at the outlet. The outflow from the selected number of cells was funneled into a little (24 cm^3) overflow pond where the concentration was measured using an ion selectrode. The chloride ion was used as a tracer. This ion is known to move similar to the nitrate ion (Reeves and Beven, 1990) which is of environmental concern due to leaching from farmlands. By using the conservative chloride ion as a tracer, a worst case scenario is elucidated because neither chemical nor microbiological removal is considered. A mixture of 8.24 g NaCl in 200 ml of tap water (25,000 mg Cl^-/l) was used as a source fluid for the slug application. The chloride outflow concentration was measured continuously using a chloride-selective electrode (AgCl) (Chloride Selectrode, F1012C1, manufactured by Radiometer, Denmark), with an HgCl-electrode (type K701, manufactured by Radiometer, Denmark) as reference, also termed a Calomel electrode. The potential difference between these two electrodes was registered on a datalogger and converted to concentrations according to a calibration curve. This curve was established by collecting water samples from the cells in question, at regular intervals over the investigation period, and determining the chloride concentration by titration.

Dye Tracing and Dissection Procedure

After the flow and breakthrough experiments, dye tracer experiments were performed in an attempt to mark the preferential pathways of water and solute. An adsorbing dye (Rhodamine B) was used to ensure that the high flow regions would be stained and the color not washed off during the experiment. A solution of 0.5 g Rhodamine B per liter was used in the experiments. The dye was added to the monoliths after the flow and the solute tracer experiments were completed. Three liters of dye tracer solution (42 mm) were applied to monolith I through the rainfall simulator at an intensity of 10 mm/h, and 23 liters (325 mm) were added to monolith II at the same rate. The monoliths were sliced either horizontally at 8 cm intervals (monolith I) or vertically (monolith II) after draining and examined for dye staining. A special technique was used for the horizontal slicing to avoid smearing of the surface and destroying the macropores: First the PVC-casing was cut open and removed gently. Then the plaster was broken off successively downwards in small pieces. In this way the monolith was dissected slice by slice without losing the lower support of the plaster. When the plaster was removed at a given dissection level, the soil was gently broken off in pieces and the appearing surface was vacuumed. This technique left the macropores open and preserved the general structure of the monolith. The vertical dissection was accomplished by a similar procedure, but in this case we tried to follow single macropores over longer distances vertically through the monolith.

To quantify the macroporosity at each horizontal slicing level in monolith I, a hand-drawn image of all visible (> 1 mm diameter) macropores was made on transparent

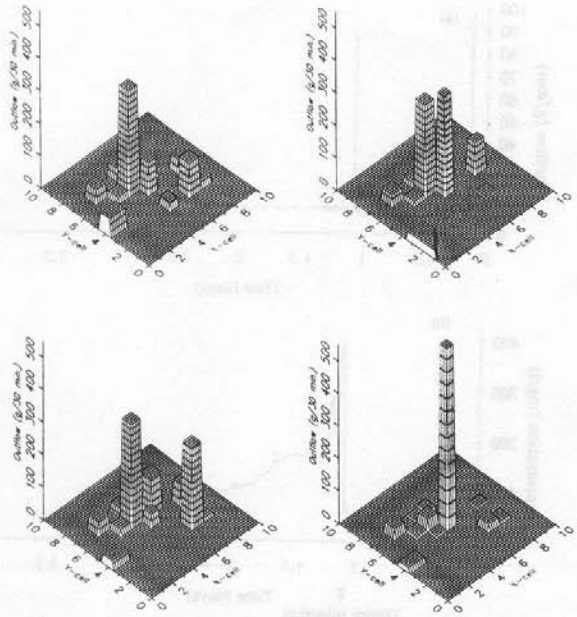

Fig. 4. Changes in outflow pattern at 30 minute intervals for monolith I after the total outflow has reached steady state. Units are grams of water per 30 min. interval.

paper. A special grid mesh was placed over the monolith surface to indicate the position of the original grid system. In this way, the base cells could be followed all the way through the monolith. An image-processing facility, PIPPIN, developed by Anakron Consult, Denmark, was used for computing digitized grey-scale pictures from a video image of the hand-drawn images. With this facility, the macroporosity was estimated as the area of all marked (visible) pores relative to the total cross-sectional area at a given dissection level. The facility is also capable of estimating the pore-size distribution at the different levels in the monoliths. The vertical slicing was only used for visual evaluation of the continuity of the macropores.

Results and Discussion

Flow and Solute Transport Experiments

The flow distribution at the bottom of the monoliths varied significantly across the outflow area and only a few cells were discharging at a given time, which is interpreted as a result of macropore flow. Furthermore, rapid temporal changes in flow pattern were observed for both monoliths, and within a 30 minute interval the flow distribution would change significantly. The results shown in Figure 4 represent the flow conditions in monolith I after the total outflow had come to steady state. We interpret the temporal changes in the flow distribution to be a result of redistribution of the entrapped air phase, which forces the water to find other pathways. Linden and Dixon (1976) have reported that even a low air pressure may block the water entry into macropores and thereby impede macropore flow.

The initiation of flow for the two monoliths at an intensity of 5 mm/h is shown in Figure 5(a) and 5(b). For both columns, outflow was initiated after approximately 0.5 days, and the average total outflow approached steady state after approximately 0.7 days, although relatively large short-range fluctuations in the outflow were still present as a result of fluctuating pathways.

When the total flow rate reached steady state, the tracer experiments were carried out, and the resulting breakthrough curves (BTCs) are shown in Figures 6-9 with the relevant outflow curves (see Figure 3 for location of individual cells). Note that in the first experiment involving monolith I the outflow was measured for the whole column, while the solute breakthrough was measured for the nine center cells. For monolith II the outflow was measured in the same subset of cells as for the solute breakthrough measurements resulting in a more appropriate representation of flow and transport relations. Also note that the concentration in the breakthrough graphs is plotted with different scaling (y-axis), and the time of tracer application is indicated by the start of the BTC. The points on the solute outflow curves marked as calibration points refer to the times at which outflow samples were collected for chloride analysis by titration to establish the calibration curve. The observed BTCs for both monoliths feature fairly early breakthrough with considerable variations in peak concentration depending on which cells were monitored. Some curves show quite extensive tailing, which together with the early breakthrough is a phenomenon related to macropore flow (Brusseau and Rao, 1990). Most of the curves have multiple peaks, although the number of peaks and the peak concentrations generally are higher for monolith I than for monolith II.

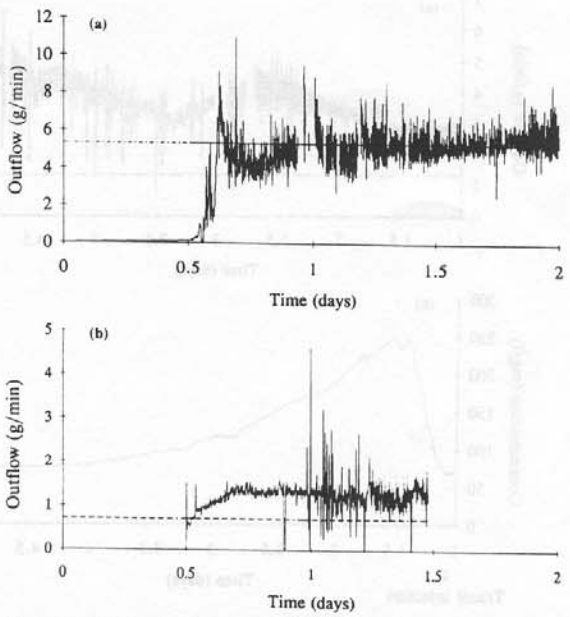

Fig. 5. Initiation of flow for 5 mm/h water application. Unit is grams of water per min. (a) Monolith I [——— total outflow, ----water application (5.13 g/min)]; (b) Monolith II [——— outflow from nine center cells, ---- water application corresponding to the area of nine cells (0.73 g/min)].

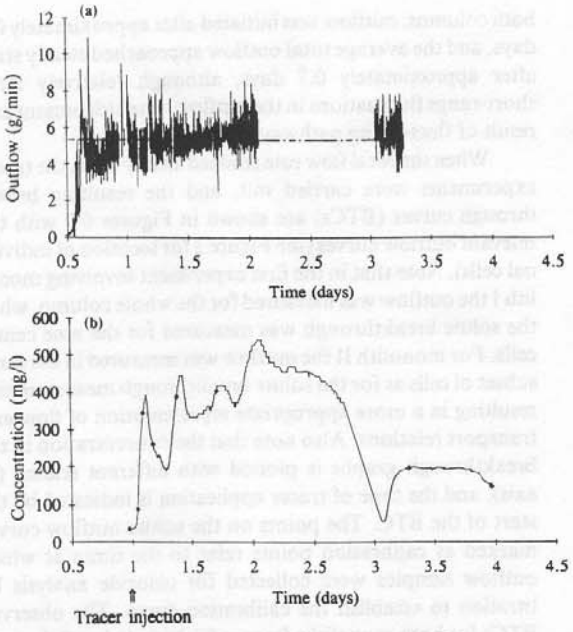

Fig. 6. Tracer experiments, monolith I, 5 mm/h. Units are grams of water per min. and mg per liter. (a) ——— total outflow (discontinuous measurements), ---- water application (5.1 g/min.); (b) ——— flux-averaged tracer concentration from nine center cells, ♦ calibration points.

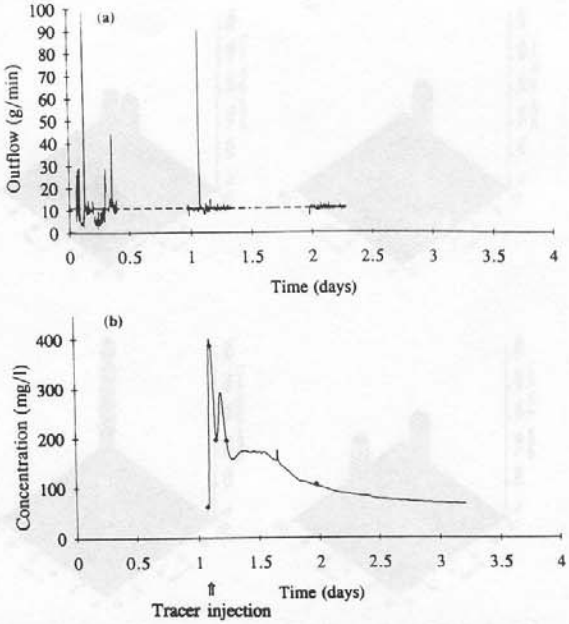

Fig. 7. Tracer experiments, monolith I, 10 mm/h. Units are grams of water per min. and mg per liter. (a) ——— total outflow (discontinuous measurements), ---- water application (10.2 g/min.); (b) ——— flux-averaged tracer concentration from nine center cells, ♦ calibration points.

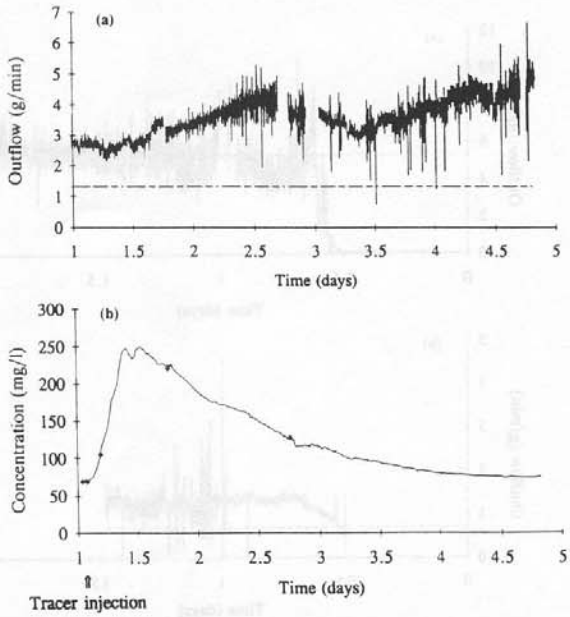

Fig. 8. Tracer experiments, monolith II, 10 mm/h. Units are grams of water per min. and mg per liter. (a) ——— outflow from nine center cells (discontinuous measurements), ---- proportional flow contribution of nine cells; (b) ——— flux-averaged concentration from nine center cells, ♦ calibration points.

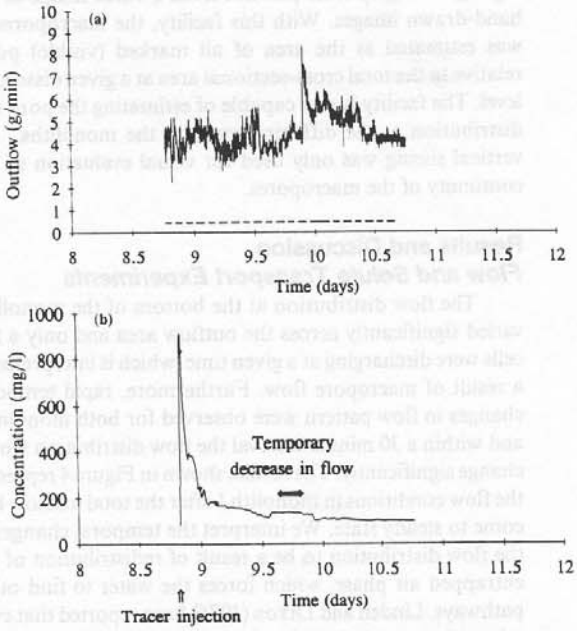

Fig. 9. Tracer experiments, monolith II, 10 mm/h. Units are grams of water per min. and mg per liter. (a) ——— total outflow from cells (3,6), (5,4) and (6,6), ---- proportional flow contribution of three cells; (b) ——— flux-averaged tracer concentration from cells (3,6), (5,4), and (6,6), ♦ calibration points.

The multiple peaks and the tailing of the observed BTCs can be attributed to different macropore phenomena. Tailing is interpreted to be a result of the process of diffusion. Following the passage of the solute front in the macropores, the matrix is considered as a diffusive source of solute with respect to the macropores (see e.g. Tyler and Thomas, 1981), and due to the slow process of diffusion, an extensive tailing results. Vertical displacement of solute from the matrix may also contribute to the tailing effect. The multiple peaks are interpreted to be a result of differences in pore size, tortuosity, and connectivity of the macropore system as well as redistribution of entrapped air. Large, well-connected macropores will transmit water and tracer rapidly, compared to small, tortuous, and less well-connected macropores. Furthermore, some macropores have dead ends leading to the process of internal catchment (Booltink and Bouma, 1991). Water and solute infiltrating from the dead ends may reach another macropore, and the flow will accelerate again. If the soil consists of a multitude of individual macropores that sometimes are connected to whole macropore networks, which in fact was documented in the dye experiments, this may explain the observed phenomena. Similar findings are reported by Andreini and Steenhuis (1990), who also carried out flow and tracer experiments on monoliths. Moreover, we hypothesize that redistribution of air entrapped in the soil may also contribute to the generation of multiple peaks. When air is displaced from one region to another, different macropores may become activated at different times which results in individual breakthrough peaks. Therefore, our interpretation of the system is that flow in macropore networks, air entrapment within these, and diffusion processes are the mechanisms responsible for the characteristics of the BTCs.

The above conclusion is supported by the following observations: Comparing the BTCs for the 5 mm/h and 10 mm/h water applications for monolith I [Figures 6(b) and 7(b)], a faster response can be observed in the 10 mm/h case (fast rise and decline). The fast response is assumed to be caused by the higher flow rate through the macropores, causing earlier breakthrough at the bottom, and faster dilution and out-washing of the solute, resulting in a faster decline at this flow rate. A comparison of the solute outflow concentration for the two different monoliths at 10 mm/h [Figures 7(b) and 8(b)] shows that monolith I responds more rapidly than monolith II. If this response is to be explained by the proposed macropore flow phenomena, the slower response should result from a macropore network consisting of smaller, less well-connected and more tortuous pores. This would account for the slower rise and decline of the BTCs in monolith II; yet, the differences in size, connectivity, and tortuosity within monolith II would still generate the multiple peaks as observed also for this monolith. The lower peak concentration in monolith II is then caused by the large degree of mixing with preexperiment water of low solute concentration which takes place in a more tortuous flow path. The difference in response time between the monoliths is supported by the observations made during the dye experiments. The stained traces indicating regions of relatively fast flow were much more dispersed and less interconnected for monolith II than for monolith I.

Figure 9 shows the results for a subset of three cells for the same experimental conditions as shown in Figure 8. Note that the proportional flow contribution from these cells is much higher than the averaged flow and that the breakthrough from the cells behaves differently from the flux-averaged behavior of the nine center cells by exhibiting a faster breakthrough with a higher peak concentration and a faster decline after the passage of the front. Figures 8 and 9 are another demonstration of the significant differences in flow and transport characteristics between the individual cells. An interesting feature of Figure 9 is the increase in solute concentration associated with the temporary decrease in flow rate. This feature can be explained as follows according to our interpretation of the system: At a specific time, the different cells contribute to the averaged curve with different solute concentrations (because of different flow paths). As flow in a cell decreases (probably the one of dominant flow, since the decrease is quite obvious), the contribution from this cell to the average solute concentration curve decreases, and the contribution from the remaining cells will dominate. When the flow returns to the dominant cell, the contribution from the remaining cells (of higher solute concentration) will again be diluted by the water coming from this cell, and the solute concentration will decrease.

The fact that the different cells at the bottom of the monoliths contribute differently to the total outflow of solute mass can be illustrated by a simple mass balance calculation. Five grams of chloride were added to monolith II in the first 10 mm/h experiment. The total mass flux from the nine center cells is estimated to 2.4 grams from the outflow and breakthrough curves, which is much larger than the proportional contribution which would be 9/69 of 5 grams equivalent to 0.7 grams.

The results obtained in these experiments correspond well with the results of the field experiments. Both rapid initial breakthrough in the subsurface drains and a prolonged leaching were observed in the field experiments by Villholth et al. (1991).

Dye Experiments

Dye experiments can be used to visualize the dominant conducting pathways for water and solute through soil. The basic assumption is that the stained regions in the soil show pathways of relatively fast flow while the flow in the unstained regions is relatively slow. We used Rhodamine B that adsorbs strongly to the soil, which obviously is a salient feature of a dye to be used for visualizing the dominant pathways. On the other hand, this introduces a filtering effect implying that only the dominating flow channels may be marked during the experiment, see e.g. Reeves and Beven (1990).

The dye tracer experiments and the subsequent dissection of the monoliths showed that Rhodamine B clearly marked the dominating pathways of flow, and the general flow patterns in a macroporous soil was also demonstrated. The dye was mainly confined to the macropores and only entered a few millimeters into the soil matrix.

A significant difference in response time of the two monoliths was observed during the dye tracer experiments. The dye appeared faster and more concentrated at the bot-

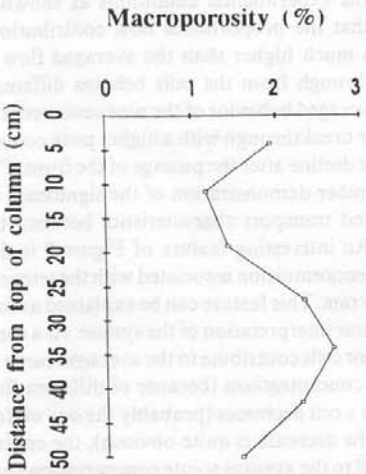

Fig. 10. Measured macroporosity for monolith I.

tom of monolith I than of monolith II, and the subsequent dissection showed that the dye was more distributed towards the bottom in monolith I than in monolith II. This was consistent with the results of the chloride tracer experiments.

The horizontal slicing showed that only in certain cases was it possible to follow individual stained macropores along the lengths of the monoliths. Both the vertical and horizontal slicing showed that macropores of similar size may have very different properties as far as water conductance is concerned, presumably due to differences in conductivity, connectivity, and tortuosity. The slicing also showed that more macropores were stained in the top layers of the monoliths in comparison to the bottom layers. This phenomenon could, to a large degree, be caused by adsorption and therefore dilution of the dye solution, but still, some dye (following the well-connected macropores) reached the bottom of the monoliths, suggesting a significant difference in the flow contribution of the pores.

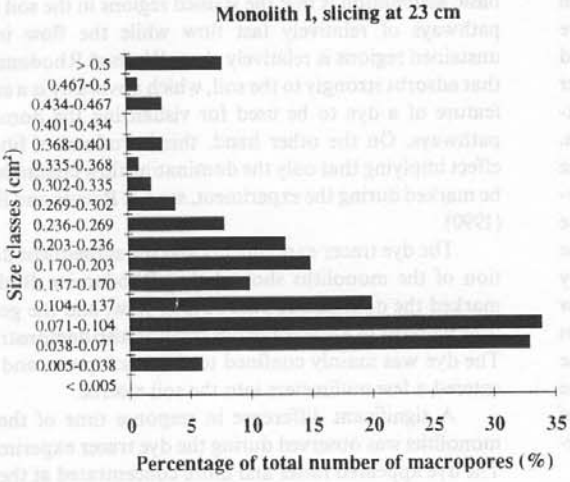

Fig. 11. Macropore size distribution.

Distribution of Macroporosity

An image-processing facility was used to determine the macroporosity of the monoliths based on a mapping of the visible macropores. The variation of macroporosity with depth for monolith I is shown in Figure 10. As shown in the figure, the macroporosity varies between 1.2 and 2.7% of the total soil surface area.

The size distribution of the macropores was estimated for the individual dissection levels by dividing the macropores mapped as described above into classes of different size. An example is shown in Figure 11 for the horizontal slicing level 23 cm from the bottom. Most of the macropores have a cross-sectional area between 0.038 and 0.170 cm^2 corresponding to a pore diameter between 2.2 mm and 4.7 mm. The size distribution for the different depths (not shown) suggests that the fraction of large pores increases with depth in the monoliths, which is in good agreement with the observations made during the monolith sectioning and the findings of Edwards et al. (1988).

Conclusions

A laboratory experimental procedure has been proposed for assessing the existence of macropores and their influence on flow and solute transport. The experiments were carried out on undisturbed soil monoliths installed in a laboratory setup in which the water application rate can be controlled. Spatial distribution of outflow, and solute breakthrough curves following a tracer injection were monitored using digital balances and selective electrodes, respectively. The procedure combines techniques, previously described in the literature, in the following way: (1) excavation of large undisturbed soil monoliths from the site for controlled laboratory investigations, (2) constant rate water application to the monoliths and measurements of the spatial distribution of the outflow, (3) tracer application and measurements of solute breakthrough curves, (4) dye injection for visual inspection of macropore transport, and (5) measurements of the distribution of macroporosity size using horizontal dissection and image processing. This sequence of experiments provides qualitative and quantitative information on the influence of macropores on flow and transport and therefore establishes a basis for selecting a suitable model for predicting flow and transport in the field.

The procedure was tested on a moraine soil typical for the eastern part of Denmark. The excavation method proved to be successful for the soil in question. In future attempts, though, it would be recommended to remove the earthworms from the monoliths after excavation. The dye-tracing technique produced somewhat questionable results because a highly sorbing dye tracer was used. Application of a nonsorbing dye tracer in combination with Rhodamine B would definitely improve the dye experiments.

The experiments showed that water and solute transport were dominated by the presence of macropores. The flow distribution was nonuniform across the outflow area, and changed rapidly with time. The breakthrough curves featured early breakthrough and in some cases extensive tailing. This type of outflow pattern is typical for macropore flow. In addition, most of the curves obtained in the break-

through experiments had multiple peaks indicating that the tracer reached the bottom of the monoliths through a variety of pathways with different travel times. The multiple peak phenomenon was confirmed by comparing the BTCs from different cells of the sampling grid. It was also hypothesized that redistribution of entrapped air contributed to this phenomenon. The dye experiments and successive sectioning demonstrated regions of relatively fast flow and that these regions were associated with discrete macropores. Thus, the experimental results provided strong evidence on the influence of macropores on flow and transport, and a numerical model should therefore include a macroporous domain in order to provide a realistic description of the transport conditions in the investigated soil.

Even though the sample size used in the study is larger than the traditional sampling size, the scale is still much smaller than the scale at which modeling is performed for field systems. To consider the scale problem arising from the heterogeneity always present in field systems, several samples from a given field site should be collected. The actual number will depend on the spatial correlation characteristics of the soil. Moreover, if the vadose zone is relatively deep, sampling over larger depth should be carried out to account for the vertical variation in soil properties. Hereby, it is possible to extrapolate the laboratory-generated data to field conditions.

References

Anderson, J. L. and J. Bouma. 1977a. Water movement through pedal soils: I. Saturated flow. Soil Sci. Soc. Am. J. v. 41, pp. 413-418.

Anderson, J. L. and J. Bouma. 1977b. Water movement through pedal soils: II. Unsaturated flow. Soil Sci. Soc. Am. J. v. 41, pp. 419-423.

Andreini, M. S. and T. S. Steenhuis. 1990. Preferential paths of flow under conventional and conservation tillage. Geoderma. v. 46, pp. 85-102.

Beven, K. and P. Germann. 1982. Macropores and water flow in soils. Water Resour. Res. v. 18, pp. 1311-1325.

Booltink, H.W.G. and J. Bouma. 1991. Physical and morphological characterization of bypass flow in a well-structured clay soil. Soil Sci. Soc. Am. J. v. 55, pp. 1249-1254.

Bouma, J. and J. L. Anderson. 1977. Water and chloride movement through soil columns simulating pedal soils. Soil Sci. Soc. Am. J. v. 41, pp. 766-770.

Brown, K. W., J. C. Thomas, and M. W. Aurelius. 1985. Collecting and testing barrel sized undisturbed soil monoliths. Soil Sci. Soc. Am. J. v. 49, pp. 1067-1069.

Brusseau, M. L. and P.S.C. Rao. 1990. Modeling solute transport in structured soils: A review. Geoderma. v. 46, pp. 169-192.

Edwards, W. M., M. J. Shipitalo, and L. D. Norton. 1988. Contribution of macroporosity to infiltration into a continuous corn no-tilled watershed: Implications for contaminant movement. J. Contam. Hydrol. v. 3, pp. 193-205.

Everts, C. J., R. S. Kanwar, E. C. Alexander, Jr. and S. C. Alexander. 1989. Comparison of tracer mobilities under laboratory and field conditions. J. Environ. Qual. v. 18, pp. 491-498.

Ghodrati, M. and W. A. Jury. 1990. A field study using dyes to characterize preferential flow of water. Soil Sci. Soc. Am. J. v. 54, pp. 1558-1563.

Ghodrati, M. and W. A. Jury. 1990. A field study of the effects of soil structure and irrigation method on preferential flow of pesticides in unsaturated soil. J. Contam. Hydrol. v. 11, pp. 101-125.

Jardine, P. M., G. V. Wilson, and R. J. Luxmoore. 1990. Unsaturated solute transport through a forest soil during rain storm events. Geoderma. v. 46, pp. 103-118.

Jarvis, N. J., L. Bergström and P. E. Dik. 1991. Modelling water and solute transport in macroporous soil. II. Chloride breakthrough under non-steady flow. J. of Soil Science. v. 42, pp. 71-81.

Khan, A.U.-H. and W. A. Jury. 1990. A laboratory study of the dispersion scale effect in monolith outflow experiments. J. Contam. Hydrol. v. 5, pp. 119-131.

Kissel, D. E., J. T. Ritchie, and E. Burnett. 1973. Chloride movement in undisturbed swelling clay soil. Soil Sci. Soc. Am. Proc. v. 37, pp. 21-24.

Kluitenberg, G. J. and R. Horton. 1990. Effect of solute application method on preferential transport of solutes in soil. Geoderma. v. 46, pp. 283-297.

Linden, D. R. and R. M. Dixon. 1976. Soil air pressure effects on volume and rate of infiltration. Soil Sci. Soc. Am. J. v. 40, no. 6, pp. 963-965.

McMahon, M. A. and G. W. Thomas. 1974. Chloride and tritiated water flow in disturbed and undisturbed soil cores. Soil Sci. Soc. Am. Proc. v. 38, pp. 727-732.

Omoti, U. and A. Wild. 1979. Use of fluorescent dyes to mark the pathways of solute movement through soils under leaching conditions: 2. Field experiments. Soil Science. v. 128, pp. 98-104.

Persson, L. and L. Bergström. 1991. A drilling method for collection of undisturbed soil monoliths. Soil Sci. Soc. Am. J. v. 55, pp. 285-287.

Reeves, A. and K. J. Beven. 1990. The use of multiple anionic tracers in the study of soil water flows: Analytical procedures. Center for Research on Environ. Systems Technical Report no. CRES/TR/9006/05.

Seyfried, M. S. and P.S.C. Rao. 1987. Solute transport in undisturbed columns of an aggregated tropical soil: preferential flow effects. Soil Sci. Soc. Am. J. v. 51, pp. 1434-1444.

Thomas, G. W. and R. E. Phillips. 1979. Consequences of water movements in macropores. J. Environ. Qual. v. 8, pp. 149-152.

Tyler, D. D. and G. W. Thomas. 1981. Chloride movement in undisturbed soil columns. Soil Sci. Soc. Am. J. v. 45, pp. 459-461.

van Genuchten, M.Th. and W. A. Jury. 1987. Progress in unsaturated flow and transport modeling. Rev. of Geophysics. v. 25, pp. 135-140.

Van Ommen, H. C., M.Th. van Genuchten, W. H. Van der Molen, R. Dijksma, and J. Hulshof. 1989. Experimental and theoretical analysis of solute transport from a diffuse source of pollution. J. Hydrol. v. 105, pp. 225-251.

Villholth, K., K. H. Jensen, and J. Fredericia. 1991. Field investigations of preferential flow behavior. Proceedings of the Symposium on Hydrological Interactions Between Atmosphere, Soil and Vegetation, Vienna 1991, International Assoc. of Hydrological Sciences. IAHS publication 204, pp. 245-261.

White, R. E. 1985. The influence of macropores on the transport of dissolved and suspended matter through soil. Adv. Soil. Sci. v. 3, pp. 95-120.

White, R. E., G. W. Thomas, and M. S. Smith. 1984. Modelling water flow through undisturbed soil cores using a transfer function model derived from ^{3}HOH and Cl transport. Soil Sci. v. 35, pp. 159-168.

Wildenschild, D. 1991. Laboratory investigations of macropore flow. Master's thesis, Institute of Hydrodynamics and Hydraulic Engineering, Technical Univ. of Denmark, Copenhagen, Denmark.